19th IMEKO TC 4 Symposium and 17th IWADC Workshop
Advances in Instrumentation and Sensors Interoperability
July 18-19, 2013, Barcelona, Spain

A frequency independent method for adaptive correction of Time Interleaved Analog to Digital Converters

Antoine Bonnetat[1, 2], Jean-Michel Hodé[1], Dominique Dallet[2], Guillaume Ferré[2]

[1] *Thales Systèmes Aéroportés S.A, 2, Avenue Gay Lussac - Centre Charles Nungesser, 78851 Elancourt, France*
[2] *IMS Laboratory, University of Bordeaux - IPB ENSEIRB-MATMECA, 351 cours de la libération, 33405 Talence Cedex, France*

Abstract-Time-Interleaved Analog-to-Digital Converters (*TIADC*) are well-known as an efficient solution to increase sampling rate. However manufacturing process introduces static errors which limit *TIADC* performance. In this paper, we propose to improve an existing method based on a fully blind digital solution using an adaptive least mean squares (*LMS)* filter to correct gain, offset and timing mismatch. Indeed, due to interpolation operation, that solution was not frequency independent. Therefore we propose a novel architecture which is still based on adaptive filtering while dealing with frequency limitation. Numerical simulation results will be provided to validate the efficiency of our method.

I. Introduction

Increasingly Analog-to-Digital Converters (*ADC*) manufacturers have to deal with a demand of device with higher sampling rate and greater resolution. However, it is well-known that conversion is not perfect in *ADC* device: added noise combined with slew rate limitation lead to rapid degradation of resolution while increasing sampling rate. Therefore, Time-Interleaved *ADC*s (*TIADC*) [1] are currently used to provide good noise characteristics at high sampling rate while keeping reasonable power consumption. *TIADC* consists of *M* interleaved *ADC*s sampling at F_s/M. This on-chip device is driven by a common analog input sampled alternately by each *ADC* which its outputs are then interleaved by a multiplexer leading to an overall sampling rate of F_s.

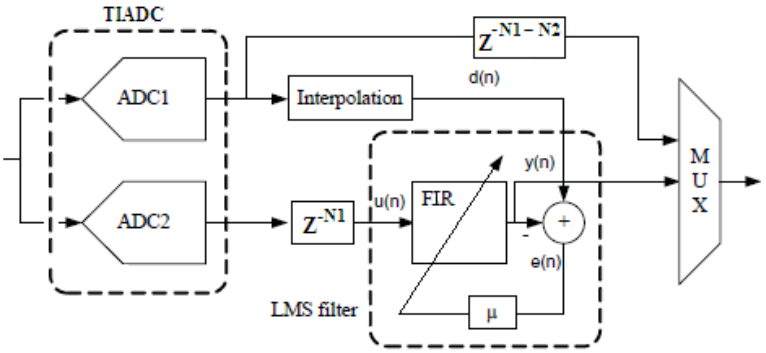

Figure 1. Former *LMS*-based correction of a dual-*TIADC*

Due to *ADC* sub-sampling, periodic images of the signal occur within the Nyquist band of the *TIADC*. Ideally these unwanted images cancel each other in interleaving *ADC*s' output signals. However, *ADC*s do not provide perfectly similar conversion characteristics due to imperfection during manufacturing process and inaccurate on-chip matching. Thus, complex gain discrepancies and clock skewing occur between *ADC*'s channels and are responsible for bad image cancelation leading to dynamic limitations, as reported in [2] and [3].
To overcome this problem, many solutions have been proposed in the literature that can be divided in two main approaches: fully digital signal processing [4]-[7] and mixed signal processing [8]-[10] (non-exhaustively).
Among signal processing solutions, a *LMS*-based adaptive gain mismatches correction has been proposed in [4]. It mainly consists (Fig. 1) in achieving feedback control of the gain of (*M-1*) channels while using the last one as a reference. Therefore reference signal interpolation is proposed for channels synchronization. However, frequency response of the interpolation filter depends on the frequency localisation of the input signal (proper Nyquist band selection) leading to system bandwidth restriction. In this paper, we propose a new architecture to overcome this problem.

ISBN-10: 84-616-5438-2 | ISBN-13: 978-84-616-5438-3

II. Description

The basic idea of this novel architecture is to replace the former interpolation process (Fig.1) by the use of a third *ADC*. This new *ADC* is used as a common reference for all channels which, then, can be feedback controlled separately using an identical *LMS* equalization process as previously [4]. In a dual-*TIADC* design, with sampling frequency F_s (Fig 2), *ADC*1 and *ADC*2 perform $F_s/2$ sampling. To supply a common reference for both channels, it is convenient for *ADC*3 to be clocked at $F_s/3$, matching alternately sampling times of *ADC*1 and *ADC*2 (Fig 3). In the more general case, a reference $(M+1)^{th}$ *ADC* clocked at $F_s/(M+1)$ ($F_s/(M-1)$ is also possible but higher than $F_s/(M+1)$) will be convenient for a *TIADC* composed of *M ADC*s with sampling frequency F_s/M. Contrary to the architecture presented in [4], the proposed method does not require any knowledge of the signal frequency, since from a frequency point of view, all signals are folded on a common $F_s/6$ bandwidth due to either $F_s/2$ (reference) or $F_s/3$ (signal) down sampling. In the time domain and for each channel, a *LMS* equalization is performed using $F_s/6$ sampled data. It could be noted that there is no frequency ambiguity between the channel data and the reference data. In fact, using only sub-sampled data to perform channel correction does not appear as a problem since the gains of the different channels are not supposed to vary with time.

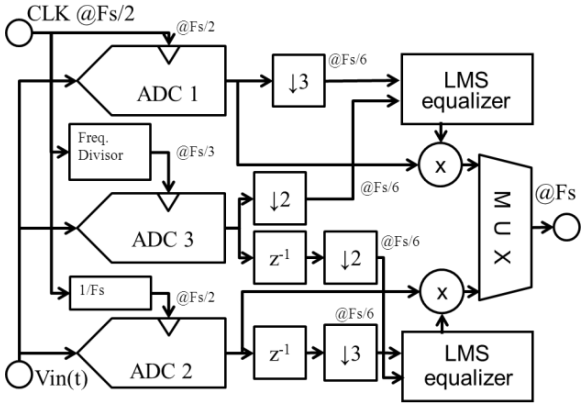

Figure 2. Proposed architecture

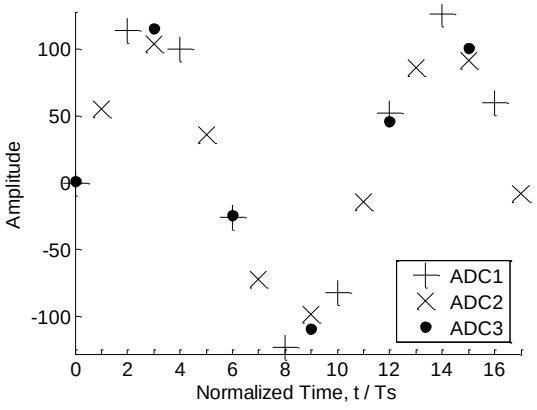

Figure 3. Sampling signal by ADC1, ADC2 and ADC3 showing alternate coincidences

III. Gain Mismatch Correction

An 8-bit 2 Gsps dual-*TIADC* (1 Gsps per channel) with 40 dB Signal-to-Noise Ratio (*SNR*), ±10% gain mismatch and no clock skew have been simulated using *Matlab* and *Simulink*. To demonstrate the ability of the proposed architecture to operate in the entire Nyquist band (contrary to previously published *LMS* structures in Fig. 1), a dual-tone signal was considered including one tone at 176 MHz (first Nyquist band of single *ADC*'s) and a second one at 613 MHz (second Nyquist band of single *ADC*'s) as presented in Fig. 4. As any feedback loop, celerity and accuracy of *LMS*-based algorithms are controlled by the effective loop gain (which is the product of the so called *LMS* step-size by the signal power).

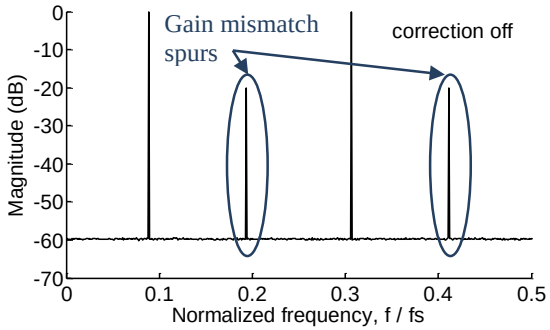

Figure 4. Dual-*TIADC* output frequency response* without correction (normalized relative to input spurs).

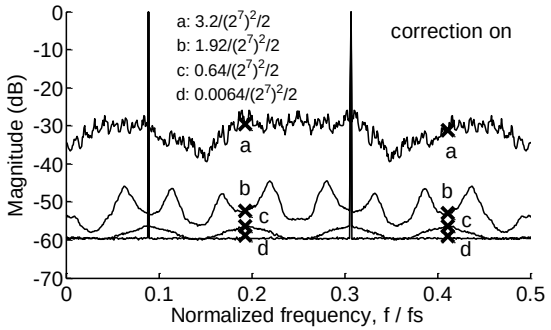

Figure 5. Dual-*TIADC* output frequency responses* after loop stabilization (four values of the effective loop gain). Crosses indicate gain mismatch spurs.

* Spectral plot are obtained with non-coherent post-integration ($N_{average}$ = 1024) for a FFT length of 1024 points.

ISBN-10: 84-616-5438-2 | ISBN-13: 978-84-616-5438-3

Four different values of loop gain were investigated (step sizes equal to 3.2, 1.92, 0.64 and 0.0064). Fig. 5 gives the spectrum magnitudes of the output signals corresponding to each of these four values. It can be seen that increasing loop gain induces greater added noise due to noise amplification and integration inside the *LMS* feedback loop. This is also clearly visible from the time dependence of the loop correction parameters (Fig. 6). However, in any of the four investigated cases, gain mismatch spurs are well cancelled after loop stabilization, at least below the noise floor density. This clearly indicates that, contrary to the former *LMS*-based correction of Fig. 1, the proposed correction algorithm is efficient even though the signal is present at the same time in both Nyquist bands of the single *ADC*'s.

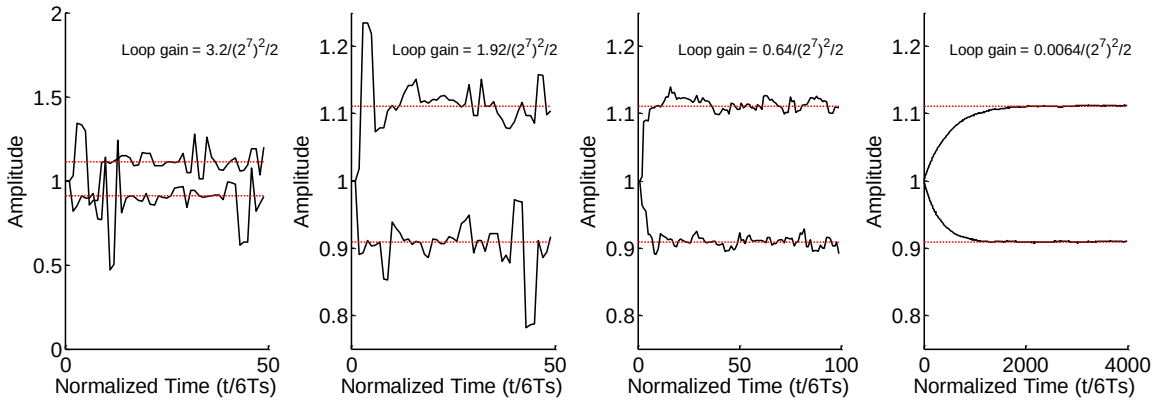

Figure 6. Time convergence of correction coefficients (same loop gains as in Fig. 5).

As can be observed in Fig. 6, reducing effective loop gain enhances convergence precision while increasing rise times. It has been noticed that noise floor density dramatically increases as loop gain approaches instability conditions. Therefore the choice of the step size is the result of a compromise between loop celerity and accuracy, while preserving loop stability; it should be kept low enough to avoid noticeable degradation of the *SNR* performance (see Fig. 7).

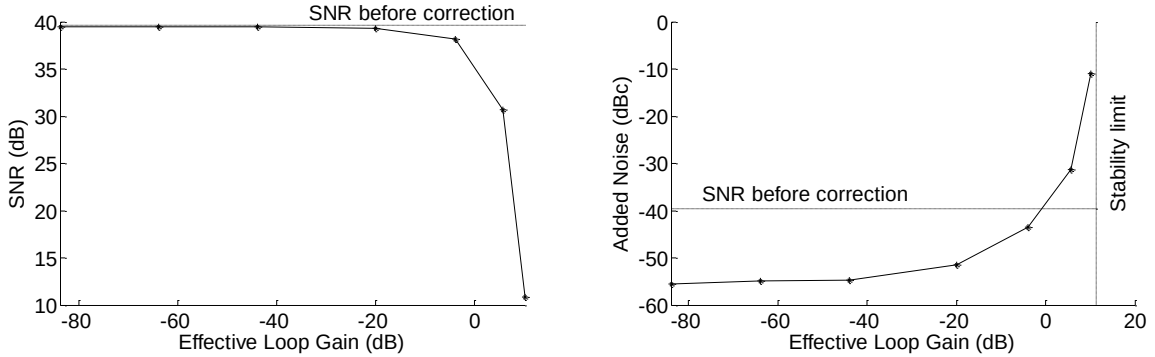

Figure 7. Influence of loop gain on *TIADC*'s *SNR* and added noise in output.

Most of published mismatch correction algorithms are only tested using single tone input signals. However, the signal spectrums may be spread over a wide band. Therefore, it is interesting to demonstrate the efficiency of the proposed algorithm with multi-tone signal covering a wide band while keeping the same gain mismatch.
First a 200 MHz-narrowband formed by hundred sinusoidal tones with random phases regularly spaced by 2 MHz was used for simulations. This signal can be centred in the first *ADC*'s Nyquist band (0-500 MHz) as illustrated in Fig. 8 or in the second one (500-1000 MHz) as illustrated in Fig. 9. It can be seen that, as for 2-tone signals, gain mismatch spurs are cancelled down to the noise floor (which is both limited by the FFT resolution and the number of tones).

ISBN-10: 84-616-5438-2 | ISBN-13: 978-84-616-5438-3

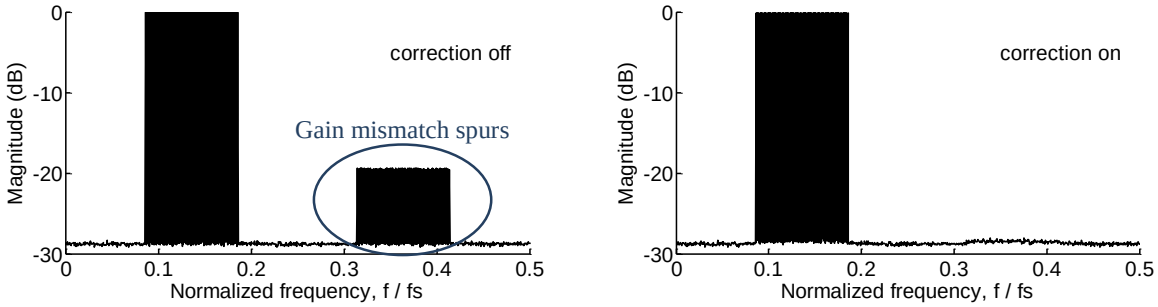

Figure 8. *TIADC* output frequency** responses with in input a narrowband in the first *ADC*'s Nyquist band

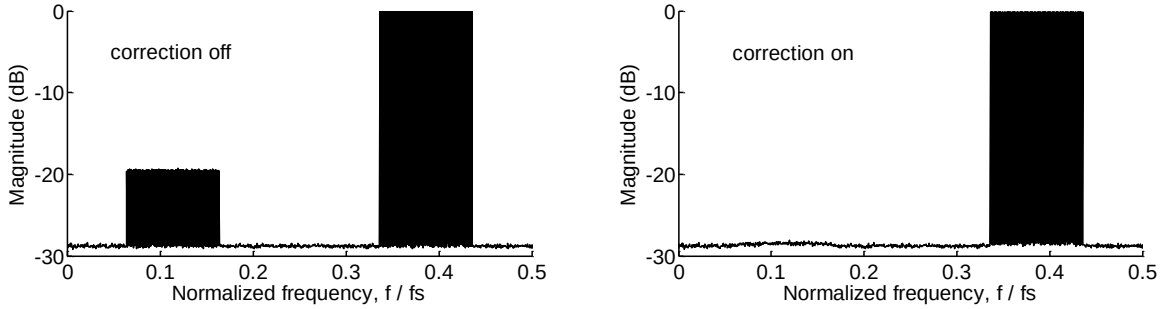

Figure 9. *TIADC* output frequency** responses with in input a narrowband in the second *ADC*'s Nyquist band

** Spectral plot are obtained with non-coherent post-integration ($N_{average}$ = 1024) for a FFT length of 2048 points.

A 19-tones signal randomly phase shifted and spread all over the first and second *ADC*'s Nyquist bands was then investigated (Fig. 10). Since the 19 tones cover the entire *TIADC* Nyquist band, the unwanted mismatch spurs (20 dB below the useful tones level before correction – plot on the left side of Fig. 10) are interleaved with useful tones. It can be seen on the right side of Fig. 10 that all these mismatch spurs are perfectly cancelled by the proposed algorithm (down to the noise floor). Indeed, since the level of the gain mismatch spurs does not depend on the input signal frequency, it is not sensitive to spectrum folding due to the sub-sampling induced by the correction algorithm.

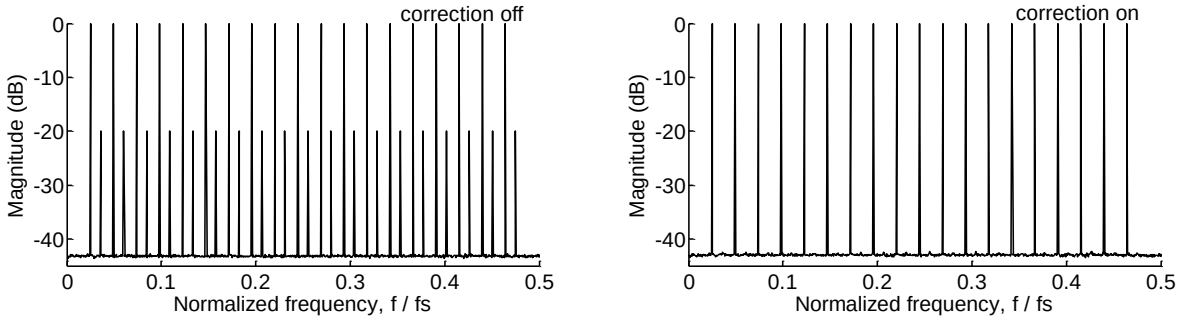

Figure 10. Frequency responses** with in input wideband spread in first and second *ADC*'s Nyquist band

** Spectral plot are obtained with non-coherent post-integration ($N_{average}$ = 1024) for a FFT length of 2048 points.

IV. Extension to correction of timing mismatch

This is no more valid for clock skew induced spurs because the level of these spurs is proportional to the signal frequency. Clock skew induced spurs cannot be cancelled by using a single coefficient but, the proposed algorithm can be extended to a finite impulse response filter (FIR) which allows compensating for clock skew mismatch. However, since the level of clock skew induced spurs depends on frequency, the method is band limited. This is due to the FIR filter, which operates at the reduced sampling rate $F_s/6$ (dual-*TIADC* case) that corresponds to the natural rate for data comparison between the ADC's and the reference *ADC*. Therefore, the input signal bandwidth should be restricted to one of the $F_s/12$ wide FIR Nyquist bands for efficient cancellation of clock skew induced spurs. Fig. 11 and 12 show simulations before correction of ±5% (relative to $T_s=1/F_s$) clock skew induced spurs for signal in the 2nd $F_s/12$ sub-band (Fig. 11) and in the 5th $F_s/12$ sub-band (Fig. 12).

Fig. 13 and 15 (respectively 14 and 16) show simulations after correction of Fig. 11 (respectively Fig. 12) data with either a 5 coefficient FIR (Fig. 13 and 14) or a 9 coefficient FIR (Fig. 15 and 16). These plots indicate that a wide band correction of timing mismatch is possible. The greater is the number of FIR coefficients, the better are spurs cancellation, as far as the signal is restricted to a single $F_s/12$ sub-band.
On the contrary, as shown on Fig. 17, it is not possible to compensate for such mismatch in the case of signals with wider bandwidth.

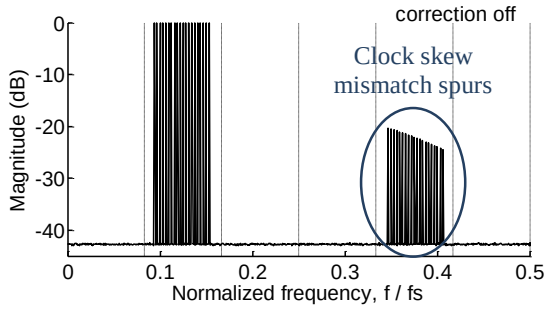

Figure 11. Frequency response** with an input signal contained in the second sub-band $F_s/12$

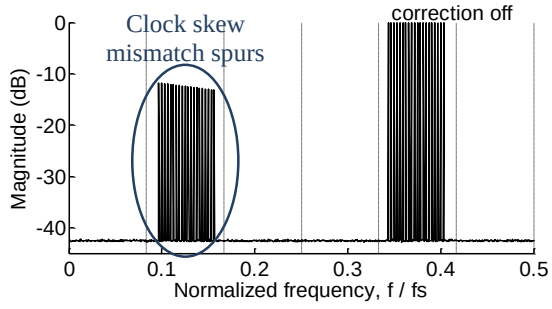

Figure 12. Frequency response** with an input signal contained in the fifth sub-band $F_s/12$

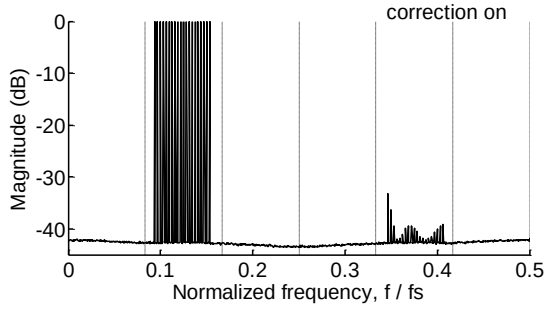

Figure 13. Frequency response** with a 5 coefficient FIR and input signal in the 2nd $F_s/12$ sub-band

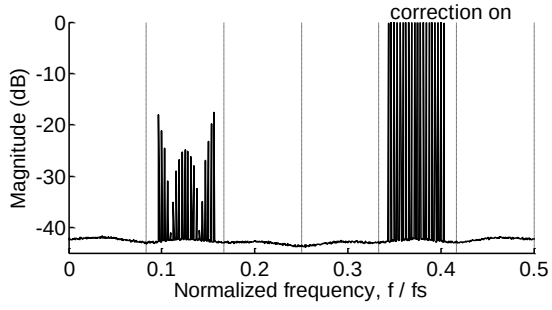

Figure 14. Frequency response** with a 5 coefficient FIR and input signal in the 5th $F_s/12$ sub-band

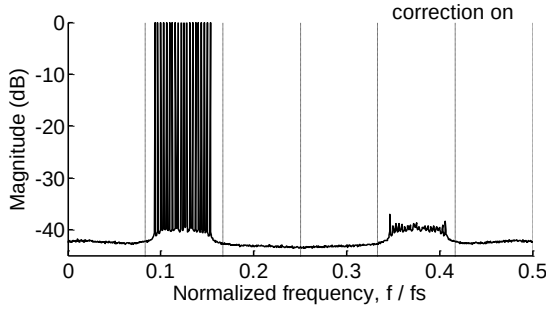

Figure 15. Frequency response** with a 9 coefficient FIR and input signal in the 2nd $F_s/12$ sub-band

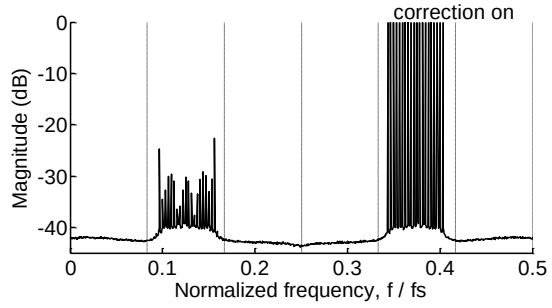

Figure 16. Frequency response** with a 9 coefficient FIR and input signal in the 5th $F_s/12$ sub-band

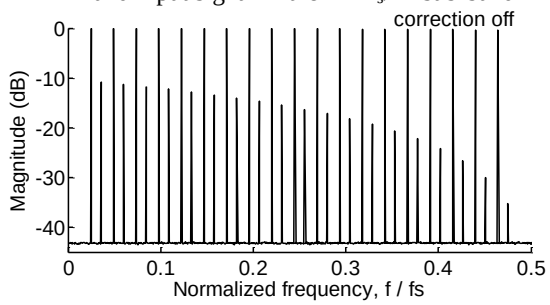

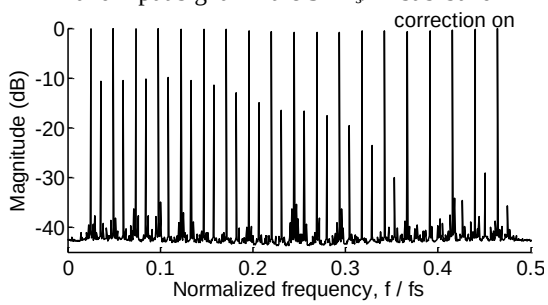

Figure 17. Frequency response** of a wideband signal spread in the entire *TIADC* Nyquist band in the case of timing mismatch (5 coefficient correction FIR)

** Spectral plot are obtained with non-coherent post-integration ($N_{average}$ = 1024) for a FFT length of 2048 points.

ISBN-10: 84-616-5438-2 | ISBN-13: 978-84-616-5438-3

V. Conclusion

A new method for adaptive correction of Time Interleaved Analog to Digital Converters has been proposed which is able to perform a frequency independent adaptive correction. An efficient spur cancellation has been observed for pure gain mismatch after loop stabilization, even if the input signal band is spread all over the entire Nyquist band of the TIADC. The dependence of loop celerity and loop accuracy as well as added noise with loop gain was studied. In addition, this method can be extended to adaptive FIR correction filters, which enables the correction of timing mismatch; in that case, the signal bandwidth should be restricted to one of the $F_s/12$ wide sub-bands. Following this condition, it is possible to reach an efficient spur cancellation; the residual spur level depends on both the number of coefficients of the FIR filter and the signal bandwidth.

References

[1] W. C. Black and D. A. Hodges, "Time interleaved converter arrays," *IEEE Journal of Solid-State Circuits*, vol. 15, no. 6, pp. 1022–1029, Dec. 1980.

[2] N. Kurosawa, H. Kobayashi, K. Maruyama, H. Sugawara, and K. Kobayashi, "Explicit analysis of channel mismatch effects in time-interleaved ADC systems," *IEEE Transactions on Circuits and Systems I: Fundamental Theory and Applications*, vol. 48, pp. 261–271, Mar. 2001.

[3] A. Petraglia and S. Mitra, "Analysis of mismatch effects among A/D converters in a time-interleaved waveform digitizer," *IEEE Transactions on Instrumentation and Measurement*, vol. 40, pp. 831–835, Oct 1991.

[4] M. Jridi, L. Bossuet, B. Le Gal and D. Dallet, "New Adaptive Calibration Method for Time Interleaved Analog to Digital Converters". *IEEE Northeast Workshop on Circuits and Systems*, NEWCAS 2007. 5-8 Aug. 2007.

[5] D. Marelli, K. Mahata, and Minyue Fu, "Linear LMS compensation for timing mismatch in time-interleaved ADCs," *Circuits and Systems I: Regular Papers, IEEE Transactions on*, vol. 56, no. 11, pp. 2476 –2486, Nov. 2009.

[6] S. Saleem and C. Vogel, "Adaptive blind background calibration of polynomial-represented frequency response mismatches in a two-channel time-interleaved adc," *Circuits and Systems I: Regular Papers, IEEE Transactions on*, vol. 58, no. 6, pp. 1300 –1310, June 2011.

[7] H. Johansson, "Compensation of Mismatch Errors in a Time-Interleaved Analog-to-Digital Converter" *Patent US7978104B2*, 2011.

[8] D. Camarero, K. Ben Kalaia, J.-F. Naviner, and P. Loumeau, "Mixed-signal clock-skew calibration technique for time-interleaved adcs," *Circuits and Systems I: Regular Papers, IEEE Transactions on*, vol. 55, no. 11, pp. 3676 –3687, Dec. 2008.

[9] G. Ferré, M. Jridi, L. Bossuet, B. Le Gal, and D. Dallet, "A new orthogonal online digital calibration for time-interleaved analog-to-digital converters," in *IEEE International Symposium on Circuits and Systems*, pp. 576–579, 18-21 May 2008.

[10] L. Rao, N. Sitthimahachaikul and P. Hurst, "Correcting the Effects of Mismatches in Time-Interleaved Analog Adaptive FIR Equalizers", *IEEE Transactions on Circuits and Systems I: Regular Papers*, 59(11), 2529 -2542. 2012.

[11] M. Zied Berriri, D. Dallet and C. Rebai, "Modeling and Performance Estimation of a Dual-TIADC", *Master Thesis*, 2009 (in French).

ISBN-10: 84-616-5438-2 | ISBN-13: 978-84-616-5438-3